Journal of Advanced Research in Fluid Mechanics and Thermal Sciences

Journal homepage:
https://semarakilmu.com.my/journals/index.php/fluid_mechanics_thermal_sciences/index
ISSN: 2289-7879

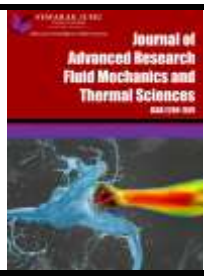

Slips and Joule Heating Impact on Heat and Mass Transfer Exploration in MHD Casson Fluid over an Exponentially Stretching Surface with Radiation Absorption

Bolla Saidi Reddy[1,*], Sabawat Hari Singh Naik[1]

[1] Department of Mathematics, University college of Science, Osmania University, Hyderabad, Telangana State, 500007, India

ARTICLE INFO

Article history:
Received 30 March 2024
Received in revised form 25 June 2024
Accepted 6 July 2024
Available online 30 July 2024

Keywords:
MHD; joule heating; nanofluid; radiation absorption; Casson fluid

ABSTRACT

In the existence of radiation absorption and Joule heating, this investigation the magnetohydrodynamic convective flow through the boundary layer of a Casson nanofluid across an exponentially inclined porous stretching surface. The PDEs are changed into a set of nonlinear ODEs by using the similarity conversions. By employing the MATLAB in built solver bvp4c, the solution to the problem is obtained. Additionally, graphical results are displayed for non-dimensional profiles. The numerical values of the Sherwood number, and Nusselt number which measure friction factor, are displayed in tabular format for diverse values of factors that regulate the flow system. To validate the obtained results, a comparison table is utilized. According to the findings, the temperature increases as a result of the thermal radiation, which also increases the effective thermal diffusivity. An increase in slip parameters is observed to result in a drop in velocity, temperature, and concentration profiles.

1. Introduction

Many processes rely on the ability of fluids to move across stretched surfaces; they include hot rolling, extrusion, metal spinning, wire drawing, and many more. To achieve a goal of quality standards, it is essential to comprehend the process's heat and flow properties. Numerous investigations have been conducted to analyze heat and fluid dynamics across a stretching sheet. These investigations have incorporated both Newtonian and non-Newtonian fluids, as well as magnetic fields and imposed electric, various thermal boundary circumstances, and a power-law fluctuation of the extending velocity. Using an exponentially extending continuous surface, Magyari and Keller [1] examined the heat and mass transport that occurs in the boundary layers. Elbashbeshy and Bazid [2] investigated the heat transfer that occurred across a continuous surface that was stretched exponentially while suction was applied. The properties of heat transport on a continuous stretched surface were investigated by Ali [3]. Pal [4] investigated the mixed convection heat transport in the boundary layers of an exponentially extending surface while taking into account the

* *Corresponding author.*
E-mail address: bollasaidireddy74@gmail.com

https://doi.org/10.37934/arfmts.119.2.5678

presence of a magnetic field. t. With the use of an exponentially extending sheet, an investigation of the hydromagnetic flow and heat transfer that occurred close to a stretched vertical sheet with a predetermined surface heat flux was carried out by Aman and Ishak [5]. In their study, Ibrahim and Shanker [6] inspected the unstable MHD boundary-layer flow as well as heat transmission that occurred as a result of extending a sheet when a heat source or sink was within the Mabood and Das [7] investigated the effects of radiation and second-order slip on the hydromagnetic flow of a nanofluid over a stretched sheet. Mukhopadhyay [8] investigated the movement of the MHD boundary level and the transport of heat across an exponentially stretched sheet that was embedded in a medium that was thermally stratified.

Under the law of viscosity, fluids may be distributed into two distinct categories: non-Newtonian fluids and Newtonian fluids. Research in this area has occurred as a result of the extensive use of non-Newtonian fluids in commercial and industrial settings. The chemical company, which includes the manufacturing of paint, shampoo, and palm oil, as well as the food sector, which includes the creation of mayonnaise, are critical uses of these sorts of fluids. Certain non-Newtonian fluids, those are Eyring-Powell fluid, and Casson fluid, are considered to be of the highest significance. The liquid known as Casson has been investigated in this research. Case studies of research that have been conducted on Casson fluid are discussed in various studies viz., Mustafa *et al.,* [9] explored the flow of a Casson fluid towards a stretched sheet, as well as the heat transfer that occurred at the stagnation point.

The Casson fluid flow close to the stagnation point across a stretched sheet of varying thickness and radiation was investigated by Ramesh *et al.,* [10]. The effects of thermal radiation and heat sources on multi-helium density Casson fluid on a vertical porous plate that oscillates were investigated by Prakash *et al.,* [11]. This study was conducted by Raju *et al.,* [12] to evaluate the outcomes of mass transmission on the MHD Casson fluid flow over an exponentially stretching sheet. Jaafar *et al.,* [13] investigated the impact of thermal radiation on the flow over an exponential stretched sheet. Dandu *et al.,* [14] investigated in the presence of chemical reaction and thermal radiation, the unsteady multi-homogeneous Casson fluid flow past a moving inclined plate embedded in a porous medium is studied using radiation absorption and diffusion thermo impacts. Kumar and Suneetha [15] examined the effects of thermal diffusion and diffusion thermodynamics on the convective flow of Williamson nanofluid through a porous medium, over a stretching surface, while subjected to chemical reactions and thermal radiation. Kataria and Patel [16] conducted research on the impact of Soret and heat generation impact MHD Casson fluid past a moving vertical plate with radiation that was immersed in a porous media. Kodi *et al.,* [17] examined the effects of chemical reactions and thermal diffusion on the flow of multi-homogeneous Casson fluids across a vertically porous plate. Hall and aligned magnetic effects were used to study MHD Casson fluid flow down an inclined plate by Kumar *et al.,* [18]. Bejawada *et al.,* [19] considered a research on the influence of chemical reaction and radiation on the stream of MHD Casson fluid on an inclined non-linear surface in a Forchheimer absorbent medium. The chemical process, the Soret and Dufour impacts, and the Casson fluid's MHD heat transport were investigated by Goud *et al.,* [20] across an exponential porous stretched surface with slip phenomena.

Because of the high temperatures that are involved in many of the processes that take place in engineering fields, having an understanding of radiation heat transmission is very crucial for the scheme of the equipment that is required. These technical specialties and the many types of propulsion systems used for aircraft and satellites. With several effects on Transient Heat and Mass Transfer in Unsteady Radiating Multi-Horizontal Flow of a Maxwell Fluid with a Porous Vertically Stretching Sheet was investigated by Annapureddy *et al.,* [21]. Radiative MHD Casson nanofluid flow and heat/mass transport across a nonlinear stretching surface were investigated by Thirupathi *et al.,*

[22]. Thermal radiation's impact on multi-hole-dipole (MHD) nanofluid flow via a stretched sheet was explored by Sulochana *et al.,* [23]. The stagnation point flow of nanofluids with different viscosities past a stretched surface heated by radiation was investigated by Makinde and Mishra [24]. Nanofluids subjected to MHD non-orthogonal stagnation point flow toward a stretched surface under heat radiation are studied by Jalilpour *et al.,* [25]. Reddy *et al.,* [26] studied how a nanofluid's hydromagnetic radiation stagnation point flow behaves when it moves across a stretched surface. Influence of Nanoparticle Shape on Aligned MHD Mixed Convection Flow of Jeffrey Hybrid Nanofluid over an Extending Vertical Plate was investigated by Awang *et al.,* [27]. The impact of mass and heat transfer on MHD flow across a porous vertical plate in the presence of chemical reactions and heat generation was investigated by Kumar *et al.,* [28].

When an electric current passes via a material that acts as a resistance, it may be said to "Joule heat" the material. light bulbs, iron clothes, Portable fan heaters, and the hot flow from hairdryers are just a few of the many uses for joule heating. Joulean dissipation, which occurs when a conducting liquid interacts with an applied magnetic field, has several practical uses. Analytical solution of unstable MHD Casson fluid with heat radiation and chemical reactivity in a porous media was investigated by Omar *et al.,* [29]. many parameters impact on Casson fluid passing a vertical plate with varying magnetic field were investigated by Vijayaragavan and Karthikeyan [30]. The impact of radiation and nanoparticle shape on aligned MHD Jeffrey hybrid nanofluid flow and heat transfer across a stretching inclined plate was investigated by Ilias *et al.,* [31]. The movement of MHD Casson nanofluid, a radiation heat source fluid, across an inclined non-linear surface with the impact of Soret and Dufour was studied by Sekhar *et al.,* [32]. A Buongiorno fluid model technique was used by Sarma *et al.,* [33] to study the MHD Casson nanofluid's behavior on inclined porosity stretching surfaces with heat source/sink and dissipation impacts. The impact of Joule heating and dissipation on MHD flow as well as heat transfer through an extended sheet immersed in an absorbent media was inspected by Swain *et al.,* [34]. With Joule heating and source/ sin impacts on mixed convection movement via an extending sheet in a Darcy-Forchheimer absorbent medium was studied by Sharma and Gandhi [35]. An exponentially expanding surface with a Joule heating, radiation was the subject of an exploration by Goud *et al.,* [36-38] into the several effects on MHD boundary layer nanofluid flow. Convective maximum heat transfer (MHD) Casson nanofluid stagnation point flow of across a porous media with chemical reaction was deliberated by Reddy *et al.,* [39] in relation to the heat source and Joule heating influences. An investigation of the Radiative MHD flow of Casson hybrid nanofluid and second-grade fluid was carried out by Krishna *et al.,* [40,41] across a semi-infinite vertical and an infinite exponentially accelerated vertical porous surface.

The goal of this research is to set out the conditions for the MHD convective boundary layer flow of a Casson nanofluid across an enormously stretched permeable stretching surface when radiation absorption and Joule heating with slip effects are present. The flow field scenario is mathematically described using PDEs and changed to ODEs with suitable conversions. When a numerical solution is required, a computational algorithm is implemented. The graphical findings illustrate the influence of the physical factors on flow profiles. Furthermore, physical quantities are calculated and made available via tables. Also, the present effort is confirmed when a good match is found when the obtained data are compared to the present values.

2. Mathematical Formulation

Take into account a nonlinearly exponentially extending sheet that corresponds with the plane $y = 0$ and a steady, incompressible, dissipative MHD Casson fluid flowing past it. At all times, the fluid flow is limited to $y > 0$. There must be no electric field and employedvarying magnetic field but

no voltage. Additional assumptions include a negligible induced magnetic field relative to the ambient magnetic field. The results suggest the presence of a low magnetic Reynolds number in this investigation. We also took into account the fuel for the flow and any chemical reactions that may occur. With the origin held still, the wall is extended by applying two opposing pressures along the x-axis. For a Casson fluid that flows in a straight line and can't be squished, the rheological equation of state is expressed as follows

$$\tau_{ij} = \begin{cases} 2\left(\mu_B + \frac{p_y}{\sqrt{2\pi}}\right) e_{ij}, \pi > \pi_c \\ 2\left(\mu_B + \frac{p_y}{\sqrt{2\pi}}\right) e_{ij}, \pi < \pi_c \end{cases}$$

Here $\pi = e_{ij}e_{ij}$ and e_{ij} are the $(i,j)^{th}$element of the deformation rate, π is the result of multiplying the deformation rate factor by itself , π_c is an important product value according to the non-Newtonian model., μ_B is dynamic plastic viscosity of a fluid that is not Newtonian, and p_y is the fluid yield stress. Figure 1 shows the physical sketched and coordinate system that was taken into consideration and the flow-governing equations may be expressed as [12]

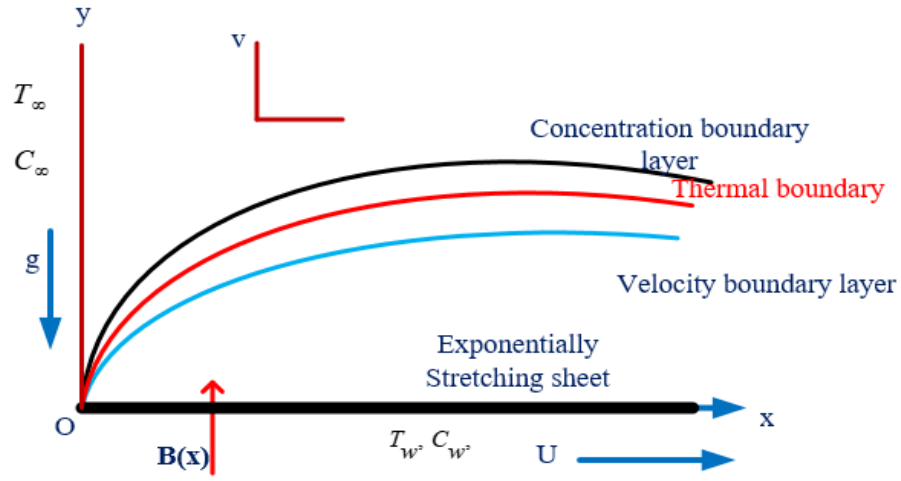

Fig. 1. Flow Geometry of the problem

$$\frac{\partial u}{\partial x} + \frac{\partial v}{\partial y} = 0, \tag{1}$$

$$u\frac{\partial u}{\partial x} + v\frac{\partial u}{\partial y} = \nu\left(1 + \frac{1}{\beta}\right)\frac{\partial^2 u}{\partial y^2} + g\beta_T(T - T_\infty) + g\beta_c(C - C_\infty) - \frac{\sigma B^2 u}{\rho} \tag{2}$$

$$u\frac{\partial T}{\partial x} + v\frac{\partial T}{\partial y} = \frac{k}{\rho c_p}\frac{\partial^2 T}{\partial y^2} - \frac{1}{\rho c_p}\frac{\partial q_r}{\partial y} + \frac{\mu}{\rho c_p}\left(1 + \frac{1}{\beta}\right)\left(\frac{\partial u}{\partial y}\right)^2 - \frac{Q}{\rho c_p}(T - T_\infty) + \frac{\sigma B_0^2}{\rho C_f}u^2 \tag{3}$$

$$u\frac{\partial C}{\partial x} + v\frac{\partial C}{\partial y} = D_m\frac{\partial^2 C}{\partial y^2} - k_l(C - C_\infty) + \frac{D_T}{T_\infty}\frac{\partial^2 T}{\partial y^2} \tag{4}$$

By using the boundary constraints

$$\left.\begin{array}{ll} u = U + A^*\left(1 + \frac{1}{\beta}\right)\frac{\partial u}{\partial y}, v = -V(x), T = T_W + B^*\frac{\partial T}{\partial y}, C = C_w + C^*\frac{\partial C}{\partial y} & at\ y = 0, \\ y \to 0, T \to T_\infty\ C \to C_\infty & as\ y \to \infty, \end{array}\right\} \tag{5}$$

Here $A^* = A_1 e^{\frac{-x}{2L}}$, $B^* = B_1 e^{\frac{-x}{2L}}$ and $C^* = C_1 e^{\frac{-x}{2L}}$ are the velocity, thermal and concentration slip factors varies with x, A_1, B_1 and C_1 are the initial value of the slip factors.

The radiative heat flow, $q_r$may be expressed using the Rosseland approximation as

$$q_r = -\frac{4\sigma^*}{3k^*}\frac{\partial T^4}{\partial y}. \tag{6}$$

Based on the assumption that the temperature variations within the flow are necessarily minimal, it is possible to describe T^4 as a function (linear) of temperature for the flow. In order to get T^4, it is necessary to expand $T^4 = 4T_\infty^3 T - 3T_\infty^4$ using Taylor series while disregarding higher order terms, In this case, Eq. (3) yields

$$\left(u\frac{\partial T}{\partial x} + v\frac{\partial T}{\partial y}\right) = \frac{k}{\rho c_p}\frac{\partial^2 T}{\partial y^2} - \frac{1}{\rho c_p}\frac{16\sigma T_\infty^3}{3\rho c_p k^*}\frac{\partial^2 T}{\partial y^2} + \frac{\mu}{\rho c_p}\left(1+\frac{1}{\beta}\right)\left(\frac{\partial u}{\partial y}\right)^2 - Q(T-T_\infty) + \frac{\sigma B^2}{\rho c_f}u^2 \tag{7}$$

A similarity conversion is now being used by us as

$$\left.\begin{array}{c} \eta = \sqrt{\frac{U_0}{2\nu L}}e^{\frac{Nx}{2L}}y,\ v = -\sqrt{\frac{\nu U_0}{2L}}e^{\frac{Nx}{2L}}N\{f(\eta)+\eta f'(\eta)\} \\ u = U_0 e^{\frac{Nx}{L}}f'(\eta), T = T_\infty + T_0 e^{\frac{2Nx}{L}}\theta(\eta), C = C_\infty + C_0 e^{\frac{2Nx}{L}}\phi(\eta) \end{array}\right\}, \tag{8}$$

Through the use of Eq. (5), Eq. (7), and Eq. (8), Eq. (2) to Eq. (4) may be converted into ODEs, which possess the form

$$\left(1+\frac{1}{\beta}\right)f''' + N(ff'' - 2f'^2) + 2Gr\theta + 2Gc\phi - Mf' = 0 \tag{9}$$

$$\frac{1}{\Pr}\left(\frac{4}{3}R+1\right)\theta'' - N(4f'\theta - f\theta') + \left(1+\frac{1}{\beta}\right)Ecf''^2 - Q_H\theta + EcMf''^2 = 0 \tag{10}$$

$$\phi'' - Nsc(4f'\phi - f\phi') - ScK\phi + \frac{Nt}{Nb}\theta'' = 0 \tag{11}$$

The transformed boundary circumstances are

$$\left.\begin{array}{c} f(\eta) = S, f'(\eta) = 1 + V_s f''(\eta),\ \theta(\eta) = 1 + T_s\theta'(\eta), \phi(\eta) = 1 + C_s\phi'(\eta),\ at\ \eta = 0, \\ f'(\eta)\to 0, \theta(\eta)\to 0, \phi(\eta)\to 0\ as \qquad \eta\to\infty \end{array}\right\} \tag{12}$$

With similarity conversions are as

$$\left.\begin{array}{c} \beta = \frac{\mu_B\sqrt{2\pi_c}}{p_y}, B = B_0 e^{\frac{Nx}{L}}, Q = Q_0 e^{\frac{Nx}{L}}, k_l = K_0 e^{\frac{Nx}{L}}, V(x) = v_0 e^{\frac{Nx}{2L}}, U = U_0 e^{\frac{Nx}{L}} \\ S = \frac{v_0}{\sqrt{\frac{U_0\nu}{2L}}}, M = \frac{\sigma B_0^2}{\rho U_0}, Gr = \frac{g\beta L T_0}{U_0^2}, Gc = \frac{g\beta L C_0}{U_0^2}, Pr = \frac{\nu_f}{\alpha_f}, R = \frac{4\sigma^* T_\infty^3}{k^* k} \\ Ec = \frac{U_0^2}{Lc_p}, Q_H = \frac{Q_0 L}{T_0 U_0}, Sc = \frac{\nu_f}{D_m}, K = \frac{k_0 L}{C_0 U_0}, Nb = \frac{\rho C_p D_B (C_w - C_\infty)}{\nu\rho C_f}, \\ Nt = \frac{\rho C_p D_B (T_w - T_\infty)}{T_\infty \nu\rho C_f},\ V_s = A_1\sqrt{\frac{U_0\nu}{2L}}, T_s = B_1\sqrt{\frac{U_0\nu}{2L}}, C_s = C_1\sqrt{\frac{U_0\nu}{2L}} \end{array}\right\}$$

where primes denote diff. with resp.to η, $S < 0$ for injection, $S > 0$ for suction.

Friction factor, Nusselt, and Sherwood number are the pertinent physical variables, and they are expressed as

$$Cf_x Re_x^{\frac{1}{2}} = \left(1 + \frac{1}{\beta}\right) f''(0)\ ,\ Nu_x Re_x^{-\frac{1}{2}} = -\theta'(0), Sh_x Re_x^{-\frac{1}{2}} = -\phi'(0) \tag{13}$$

3. Code Validation

In order to confirm the methodology used in this research and to evaluate the exactness of the current study, a contrast is made with the existing data that corresponds to the Nusselt number - θ'(0) for the Prandtl number. This assessment has been made to evaluate the correctness of the present investigation. For the purpose of drawing comparisons between the three investigations, the results are added together as shown in Table 1, which utilizes the data from Maryari and Keller [1], Pramanik [42], and Ishak *et al.,* [43]. The anticipated level of accuracy is shown by it.

4. Numerical Method

Through the use of the bvp4c scheme, the changed set of ODE Eq. (6) and Eq. (7) as well as the required boundary conditions (8) were successfully evaluated numerically. It is possible to use the programming pattern known as the boundary constraints to figure out three hidden variables. To achieve the level of precision that is needed, the operation will be carried out. Through the use of appropriate substitution, reduce each of the Eq. (8) and Eq. (9) to a set of first-order equations, which may be stated as:

$$z(1) = f(\eta),\ z(2) = f'(\eta),\ z(3) = f''(\eta),\ z(4) = \theta(\eta),\ z(5) = \theta'(\eta),\ z(6) = \phi(\eta),\ z(7) = \phi'(\eta)$$

Now, equations of the first order are given by

$$\begin{pmatrix} z'(1) \\ z'(2) \\ z'(3) \\ z'(4) \\ z'(5) \\ z'(6) \\ z'(7) \end{pmatrix} = \begin{pmatrix} z(2) \\ z(3) \\ -\frac{\begin{pmatrix} N\left(z(1)*z(3)-2*\left(z(2)\right)^2\right) \\ -M*z(2)+2*Gr*z(4)+2*Gc*z(6) \end{pmatrix}}{(1+1/\beta)} \\ z(5) \\ \left(\frac{-\mathrm{Pr}}{1+\frac{4R}{3}}\right)\begin{pmatrix} N*\left(4*z(2)*z(4)-z(1)*z(5)\right)-Qh*z(4) \\ +\left(\left(1+\frac{1}{\beta}\right)+M\right)Ec*z(3)^2 \end{pmatrix} \\ \mathcal{F}(7) \\ N*Sc*\left(4*z(2)*z(4)-z(1)*z(5)\right)+Sc*K*z(6)-z'(6) \end{pmatrix}$$

Initial circumstances that are related with this are

$$\begin{pmatrix} z_a(1) \\ z_a(2) \\ z_a(4) \\ z_a(6) \\ z_b(2) \\ z_b(4) \\ z_b(6) \end{pmatrix} = \begin{pmatrix} S \\ 1 + V_s z_a(3) \\ 1 + T_s z_a(5) \\ 1 + C_s z_a(7) \\ 0 \\ 0 \\ 0 \end{pmatrix}$$

To fulfill the criteria for convergence of 10^{-4} in the present work, a step with a size of 0.01 is established. The outcomes are derived with a precision of six decimal places.

To ascertain the dependability of our results, we conducted a comparative analysis of the flow quantities with those previously reported in research (refer to Table 1). As evidenced by the data in the tables, the results generated by the current source code are found to be considerably comparable to the published results.

Table 1
Comparison of values of $-\theta'(0)$with previous outcomes when $N = 1; Gr = Ec = M = Ec = Qh = Q_1 = 0$

Pr	R	M	Maryari and Keller [1]	Pramanik [42]	Ishak *et al.,* [43]	Present study
1	0	0	0.9548	0.9547	0.9548	0.98548
2				1.4714	1.4715	1.4715
3			1.8691	1.8691	1.8691	1.8691
5			2.5001	2.5001	2.5001	2.5001
10			3.6604	3.6603	3.6604	3.6604

5. Results and Discussion

Applying the efficient method, namely, the MATLAB inbuilt solver bvp4c with consistent guessing, the governing Eq. (9) to Eq. (11) with boundary constraints (12) are computed numerically until the boundary constraints at infinity are fulfilled. An assortment of factors that characterize the flow are subjected to numerical calculations; the outcomes are visually represented through graphs.

The difference in the velocity graph with regard to the Grashof number is seen in Figure 2. The influence of Gr, and it has been discovered that the velocity profile rises when Gr is present in high values. As anticipated, an increase in velocity is noted as a result of the strengthening of the thermal buoyancy force. Additionally, as Gr raises the velocity experiences a transition to the free stream velocity after increasing near the permeable plate.

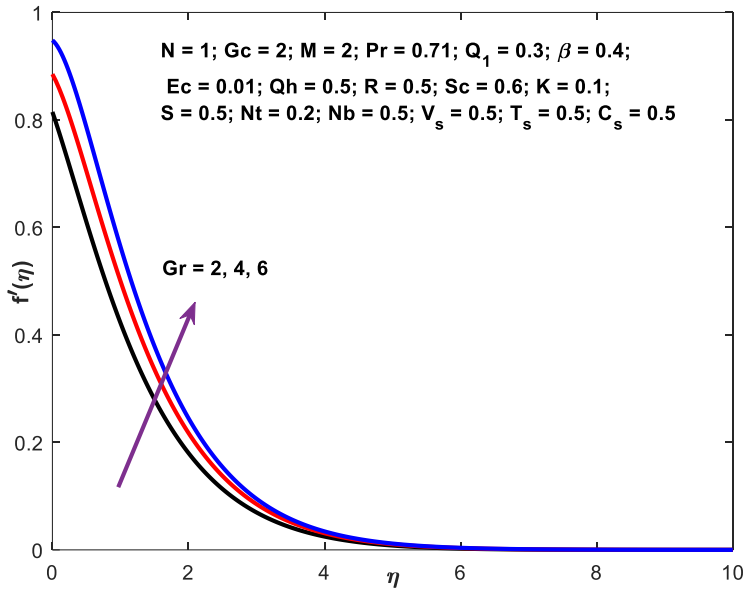

Fig. 2. Velocity profile vs Gr

Figure 3 illustrates the temperature curves corresponding to various values of the Grashof number. The figure illustrates that as the Grashof number rises, there is a corresponding drop in temperature within the thermal boundary layer. The result suggests a thinner thermal boundary layer. This is due to the buoyancy force enhancing the liquid velocity and the boundary layer width as Gr an upsurge.

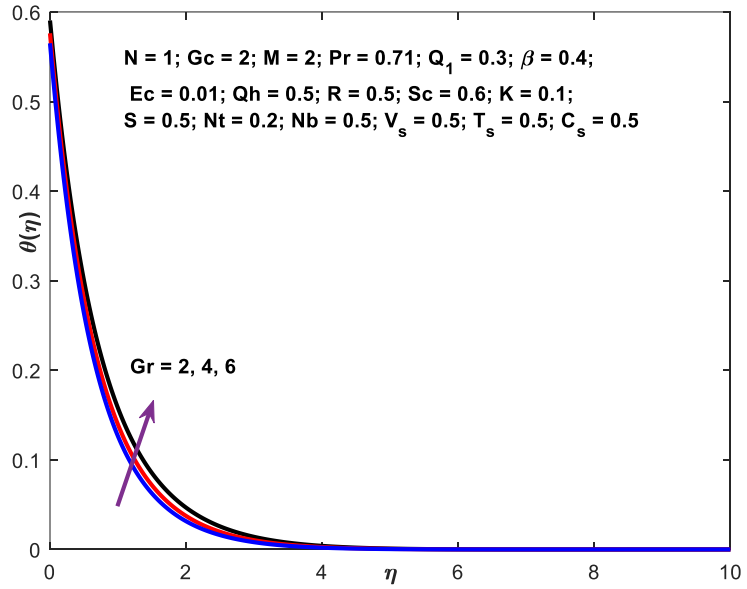

Fig. 3. Temperature profile vs Gr

Figure 4 illustrates the temperature profiles corresponding to numerous values of the Solutal Grashof number. An upward trend in the velocity curves is evident as the value of Gc enhances, as represented in the figure.

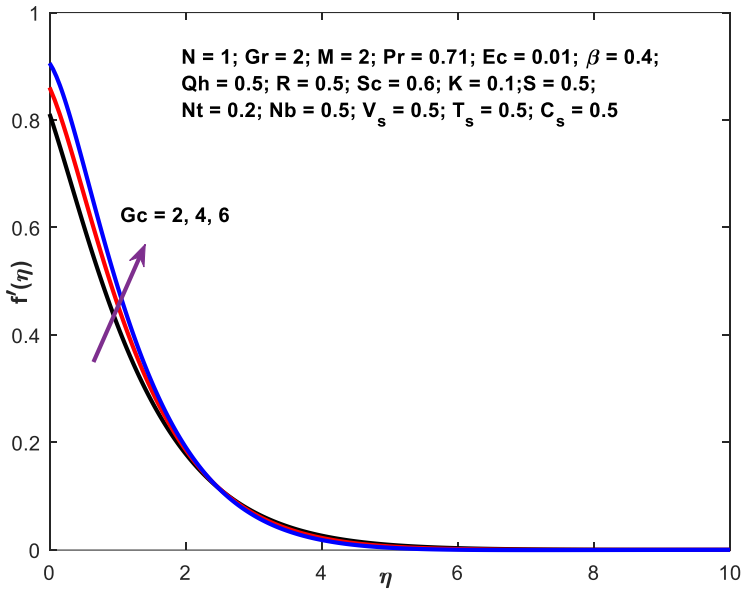

Fig. 4. Velocity profile vs Gc

For various values of the magnetic field parameter(M), the velocity outline is illustrated in Figure 5. It has been perceived that as M increases, the velocity curves decrease. The physical effect of M going up is that the boundary layer is getting thinner, which means that the speed difference is getting bigger.

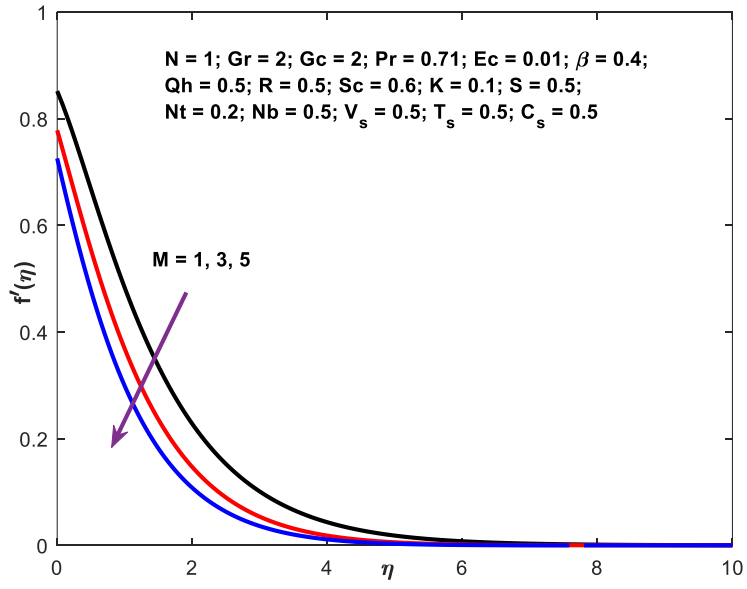

Fig. 5. Velocity profile vs M

Figure 6 and Figure 7 illustrate the effect of the parameter associated with the magnetic field (M) on the thermal and solutal boundary layers, respectively. The illustrations indicate that the thermal and solid boundary layers expand in width as M increases. This phenomenon is caused by a force working against the flow, known as the Lorentz force, which results in a fall in velocity profiles in a fluid with electrical conductivity.

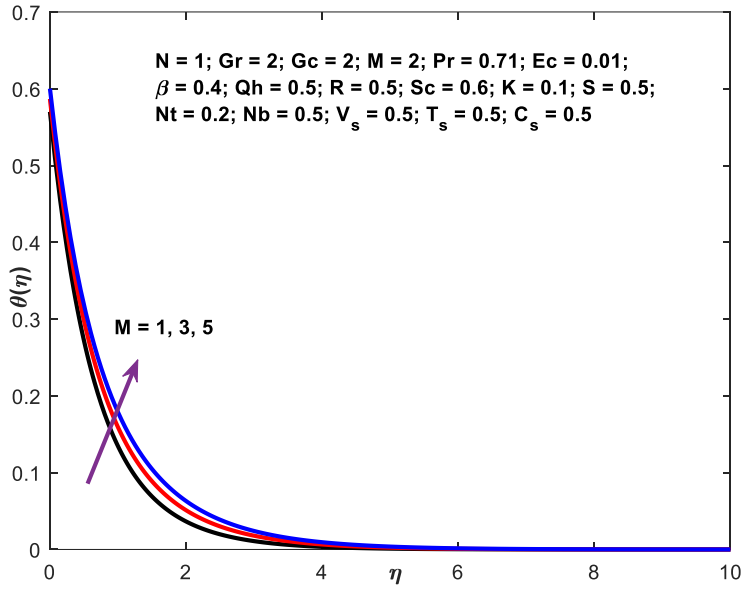

Fig. 6. Temperature profile vs M

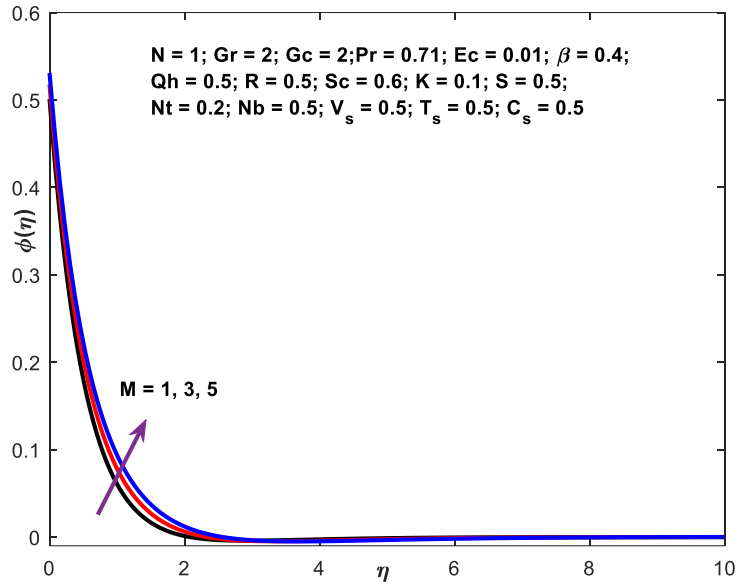

Fig. 7. Concentration profile vs M

The fluctuation of fluid temperature with regard to the Prandtl number Pr is illustrated in Figure 8. The temperature of the fluid declines as the value of Pr goes up, as illustrated by the graph. This effect happens because fluids with greater Prandtl numbers have relatively low thermal conductivities. This reduces conduction and, in turn, the temperature boundary layer's breadth, causing the temperature to drop.

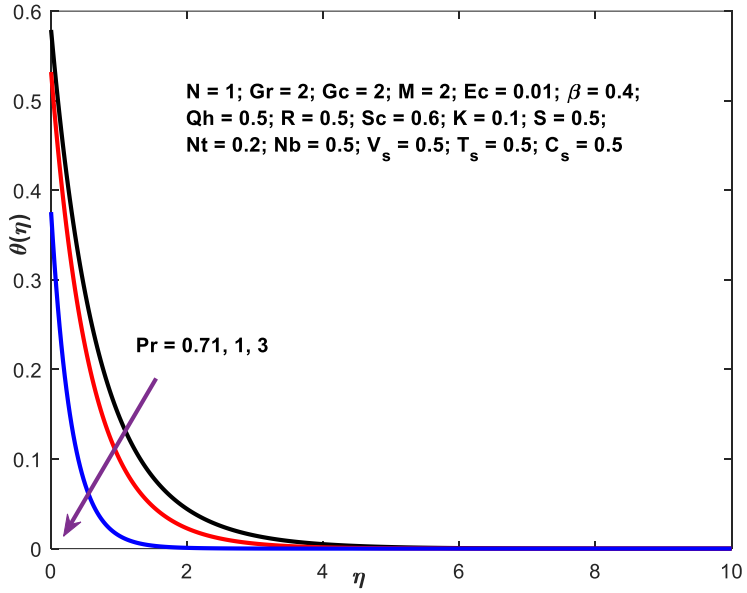

Fig. 8. Temperature profile vs Pr

Figure 9 shows the impact of the radiation component on the temperature gradients. A thicker thermal boundary layer is seen in relation to an upsurge in the radiation component.

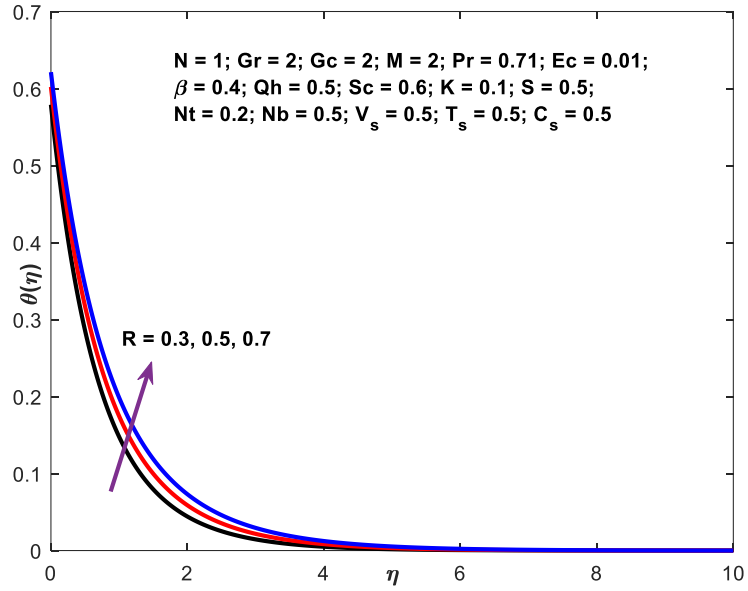

Fig. 9. Temperature profile vs R

Figure 10 illustrates the behavor of the Casson coefficient on the velocity gradient. The velocity profile is shown to decline with high values of the Casson variable. This behavior arises from the fact that increasing the Casson factor values reduces the yield stress, which is accomplished by increasing fluid viscosity. The momentum barrier layer becomes thinner as a consequence.

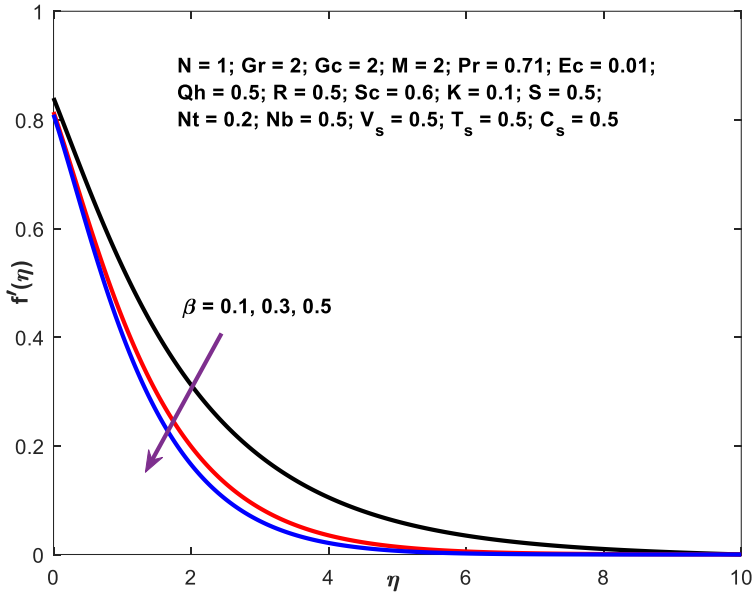

Fig. 10. Velocity profile vs β

Figure 11 to Figure 13 show how the exponential parameter affects flow patterns. The graphs clearly show that as the exponential constant goes up, the motion, temperature, and concentration border layer go down. The declining shape of the flow profiles as N, the exponential factor, increases causes this to happen. This might be because, for positive values of the exponential component, the wall temperature drops over the boundary layer, allowing the particles to disperse from the wall into the near fluid via heat transfer.

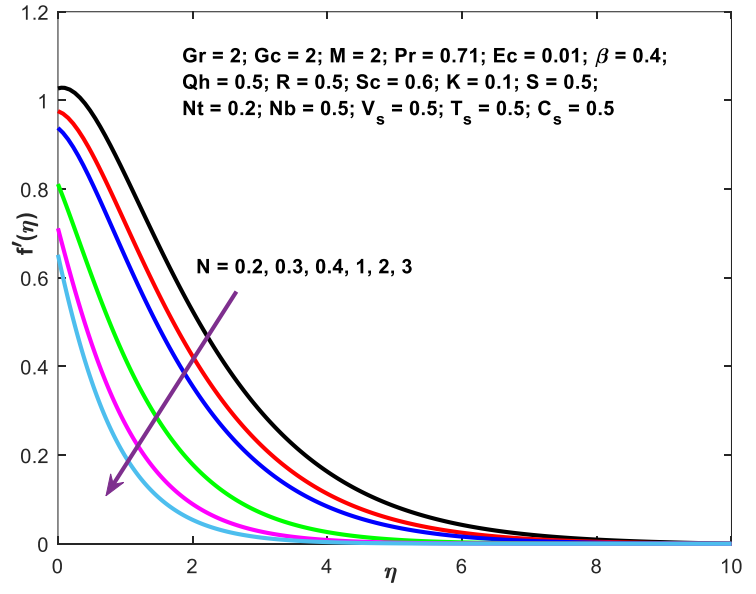

Fig. 11. velocity profile vs N

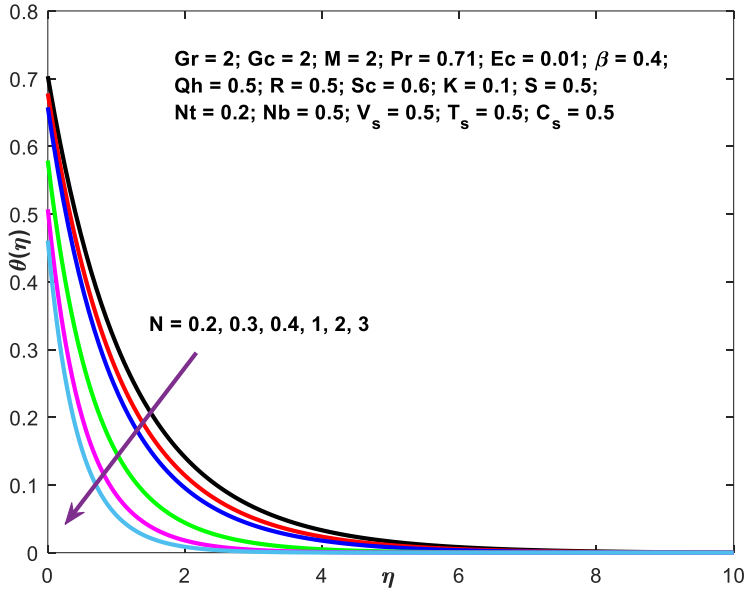

Fig. 12. Temperature profile vs N

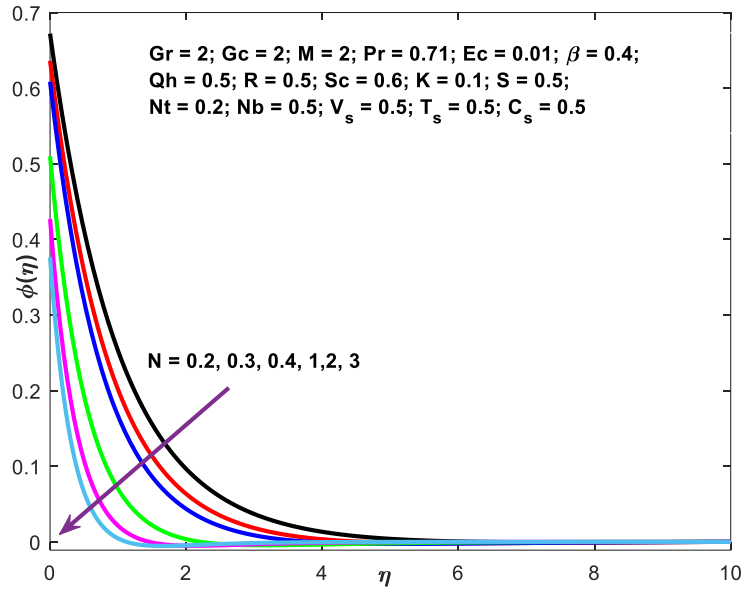

Fig. 13. Concentration profile vs N

Figure 14 depicts the Eckert number's impact on the temperature gradient. An improvement in the temperature profile is shown by an increase in the viscous dissipation factor in this example. This occurs because, due to frictional heating, heat energy is transferred to the fluid.

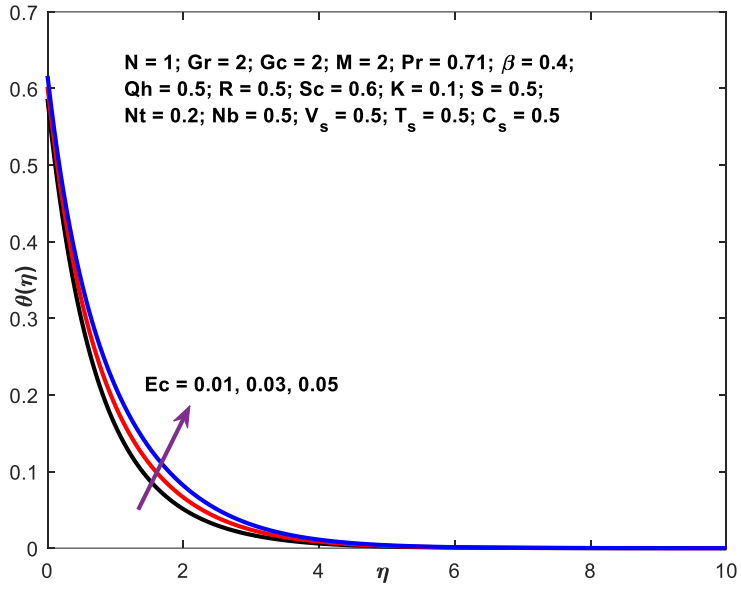

Fig. 14. Temperature profile vs Ec

Figure 15 displays the relationship between the heat source's physical behavior and the velocity profile. As may be seen from the graph, velocity curves exhibit a decline with rising Q values.

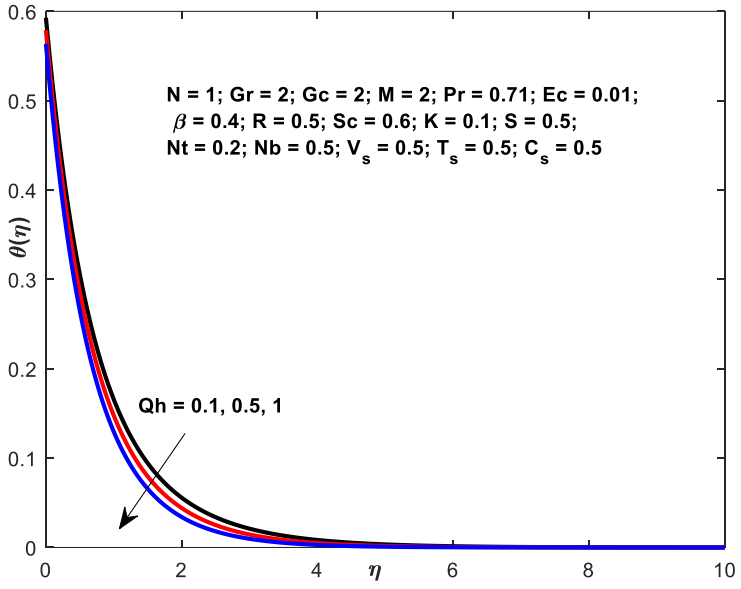

Fig. 15. Velocity profile vs Qh

Figure 16 verifies the inverse association between the Schmidt number Sc and mass diffusivity. There is a decline in the amount of mass diffusivity as the values of Sc goes up.

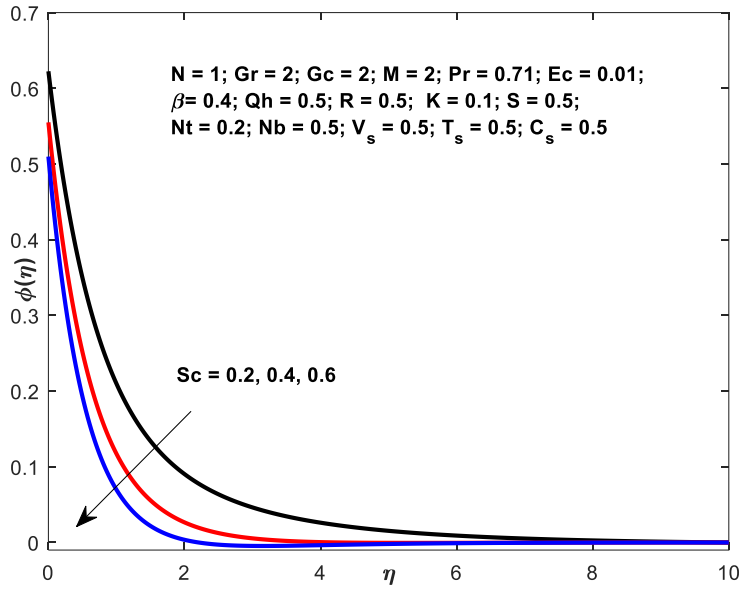

Fig. 16. Concentration profile vs Sc

The chemical reaction parameter K is shown to have a physical behavior in relation to the concentration field in Figure 17. Specifically, it exhibits that the concentration curves diminish as the K value enhances.

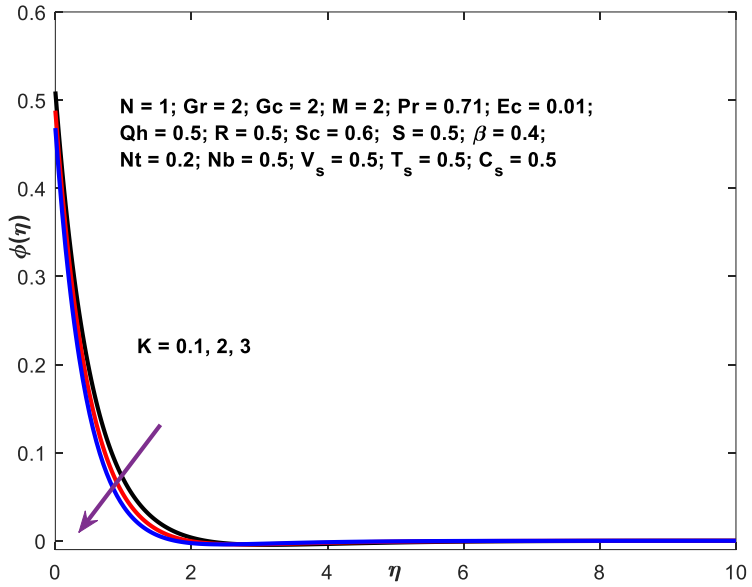

Fig. 17. Concentration profile vs K

A change in the thermophoresis parameter Nt causes the concentration graph, as revealed in Figure 18, to fluctuate. As the value of the Nt parameter goes up, so does the width of the concentration border layer. This means that the Nt parameter has a steady effect on the concentration gradient.

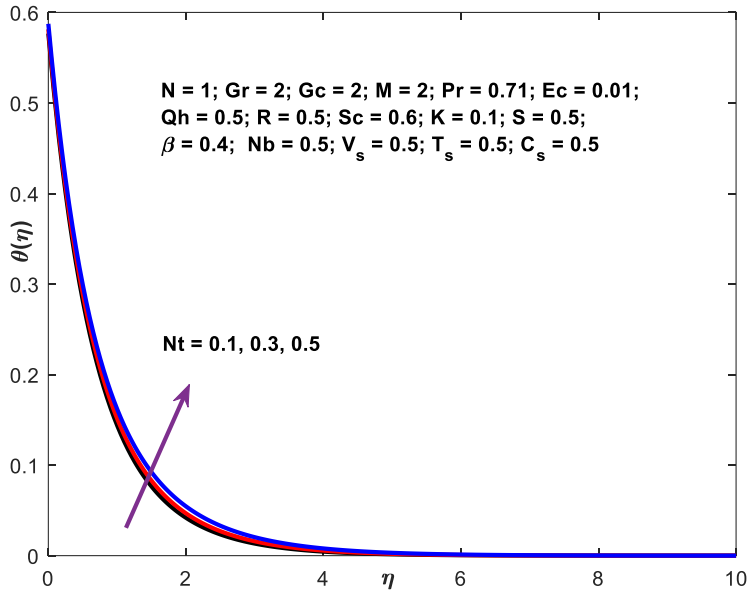

Fig. 18. Concentration profile vs Nt

Figure 19 demonstrations the concentration variation of the Brownian motion variable Nb. Increasing values of the Nb factor outcome in an increasing concentration boundary layer width.

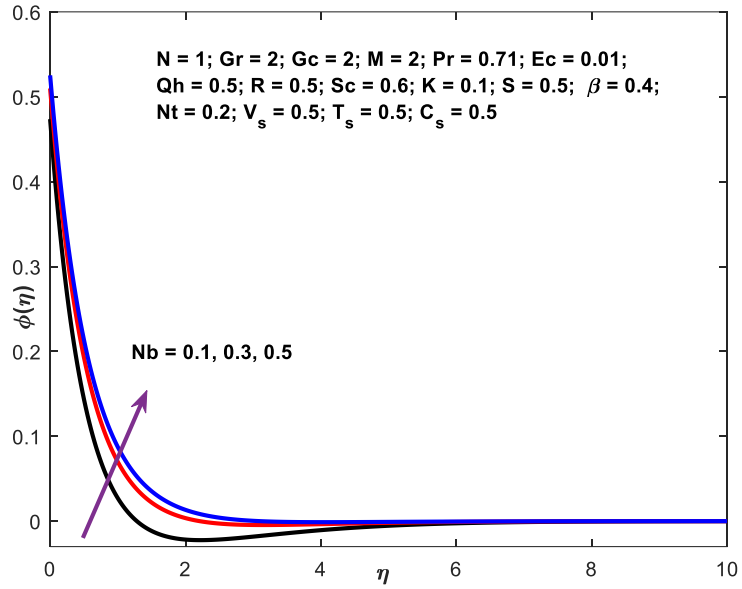

Fig. 19. Concentration profile vs Nb

The velocity profile differs in relation to the change in the suction parameter S, as shown in Figure 20. Looking at these figures, you can see that the velocity profile graph decreases as S values go higher.

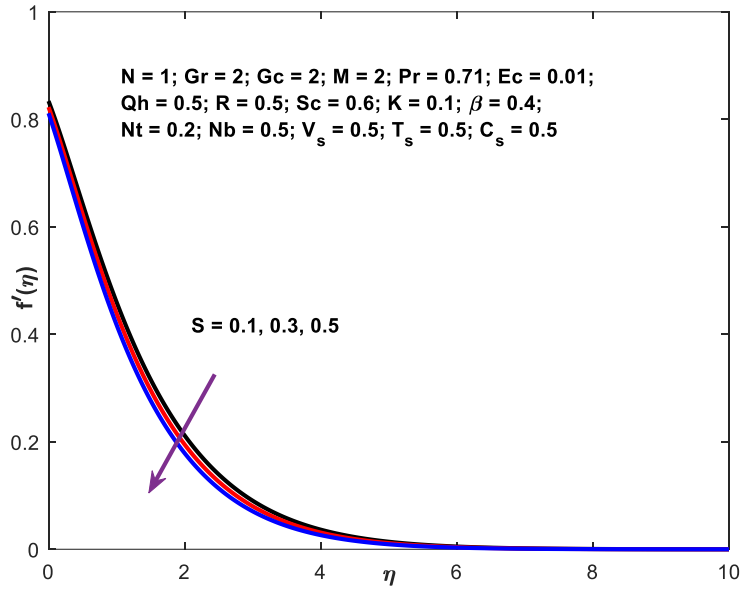

Fig. 20. Velocity profile vs S

Figure 21 shows the temperature verses velocity slip relationship. Increasing values of V_s cause a declining trend in the thermal gradient. Both the surface temperature and the width of the temperature boundary layer are falling.

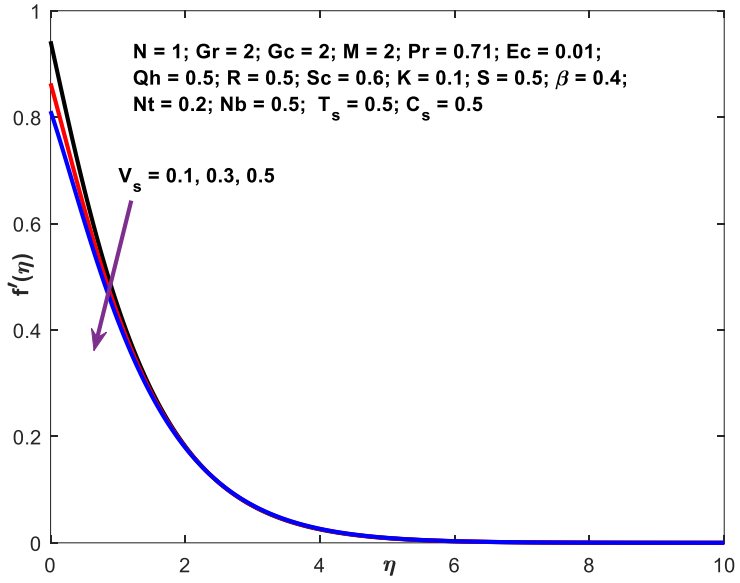

Fig. 21. Velocity profile vs V_s

The temperature profile is strongly affected by the thermal slip parameter T_s, as seen in Figure 22. As the size of the T_s upsurges, the concentration graph decreases in direct proportion to it. The relationship between the Concentration slips physical behavior on concentration filed is exposed in Figure 23. The graph clearly shows that when C_s values grow, Concentration curves declines.

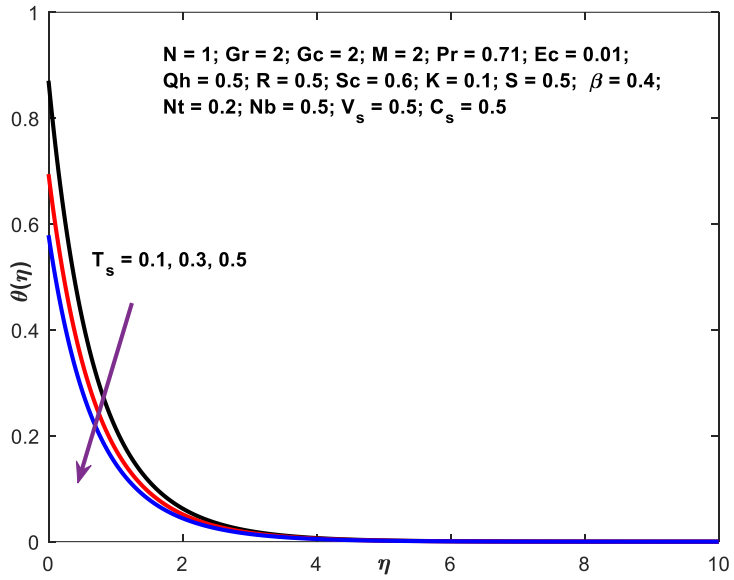

Fig. 22. Temperature profile vs T_S

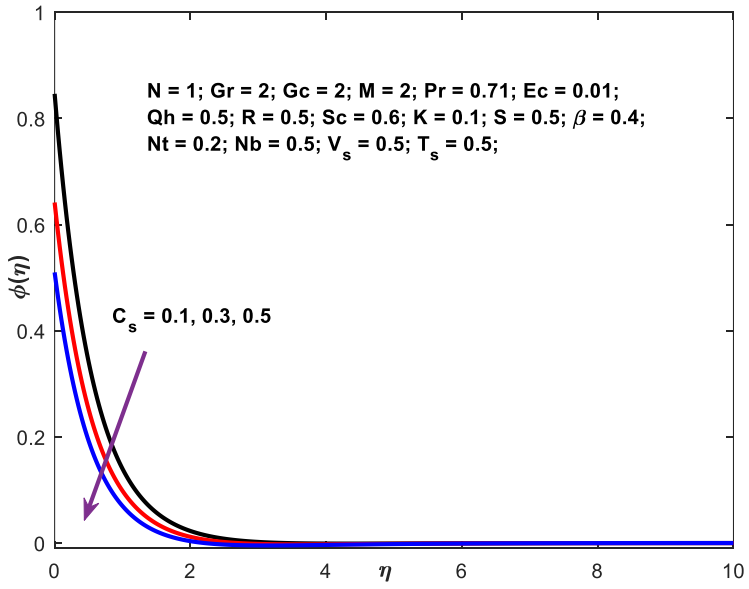

Fig. 23. Concentration profile vs C_v

Discrepancy of skin friction coefficient with the parameterGr, Gc, M, S and β is given in Table 2. An increase of Gr, M, S parameter would lead to an increase in friction factor and decrease with increase of Gc, β.

Table 2
Variations of $-(1+1/\beta)f''(0)$ with Gr, Gc, M, β, S and the other parameters are $N=1;\ Pr=0.71;\ R=0.3;\ Ec=0.01;\ Qh=0.1;\ Sc=0.2; K=0.1; Nb=0.1; Nt=0.1. V_s=0.5, T_s=0.5\ C_s=0.5$

Gr	Gc	M	β	S	$-(1+(1/\beta)*f''(0)$
1	1	1	0.1	0.1	3.412593
2					2.949370
3					2.511909
1	2				3.186988
	3				2.974257
	1	2			4.008373
		3			4.498160
		1	0.3		1.666004
			0.5		1.219467
			0.1	0.3	3.517045
				0.5	3.621403

Variation of temperature gradient with respect to $Pr, Nt\ Nb\ Ec$ and Qh, parameter is presented in Table 3. From this table, we can see that an increase of Pr, Nb, Qh parameter would lead to an escalation in the Nusselt number and decrease with enhanced values of Nt, Ec .

Table 3
Variations of $-\theta'(0)$ with Pr, Nt, Nb, Ec, Qh and Q_1, the other parameters are $N=1;\ Gr=1;\ Gc=1;\ M=1;\ R=0.3;\ \beta=0.1;\ QSc=0.2; K=0.1; S=0.1; V_s=0.5, T_s=0.5\ C_s=0.5$

Pr	Nt	Nb	Ec	Qh	$-\theta'(0)$
0.71	0.1	0.1	0.01	0.1	0.799358
1					0.887326
3					1.174509
	0.3				0.733220
	0.5				0.669970
		0.3			0.809585
		0.5			0.811406
			0.03		0.794989
			0.05		0.790664
			0.01	0.3	0.813486
				0.5	0.826846

Variation of mass transfer rate with respect to $Nt, Nb\ Sc$, and K parameter is presented in Table 4. From this table, one can perceive that an increase of Nt, Sc, K parameter would lead to a rise in the Sherwood number and decrease with enhance of Nb.

Table 4
The variation of $-\phi'(0)$ with Nt, Nb, Sc and K and the other parameters are$N = 1;\ Gr = 1;\ Gc = 1;\ M = 1;\ Pr = 0.71;\ R = 0.3;\ Ec = 0.01;\ \beta = 0.1;\ Qh = 0.1;\ S = 0.1; V_s = 0.5, T_s = 0.5\ C_s = 0.5$

Nt	Nb	Sc	K	$-\phi(0)$
0.1	0.1	0.2	0.1	0.952991
0.3				1.745927
0.5				2.494939
	0.3			0.706533
	0.5			0.657418
		0.4		1.031678
		0.6		1.088112
		0.2	0.3	0.957342
			0.5	0.961678

6. Conclusions

The purpose of the numerical research is to investigate the impacts of radiation and Joule heating on the MHD heat and mass transmission boundary layer stream of nanofluid that is propagating across a stretched sheet. For the purpose of solving the resultant system of coupled nonlinear ODEs with boundary circumstances, the numerical schema is taken into account. Due to the findings of the inquiry

i. Velocity increase of Gr, Gc and declines with an increase of M, β, N, Qh and S.
ii. Temperature profile escalation with an enhance of M, R, Ec and drops with enhance of Gr, Pr, N, and S.
iii. Concentration profile upsurge with an increase of M, Nt and declines with an enhance of N, Sc, K, Nb and S.
iv. Friction factor recedes only when Gc, βrises, while it is upsurge directly with $Gr, M$and S.
v. Nusselt number improves in direct relation to Pr, Nb and Qh, but it diminishes against Nt, Ec.
vi. Whereas the Sherwood number grows in direct proportion to Nt, Sc, and K, it decreases in relation to Nb.

Acknowledgement
This research was not funded by any grant.

References
[1] Magyari, E., and B. Keller. "Heat and mass transfer in the boundary layers on an exponentially stretching continuous surface." *Journal of Physics D: Applied Physics* 32, no. 5 (1999): 577. https://doi.org/10.1088/0022-3727/32/5/012
[2] Elbashbeshy, E. M. A., and M. A. A. Bazid. "Heat transfer over an unsteady stretching surface." *Heat and Mass Transfer* 41 (2004): 1-4. https://doi.org/10.1007/s00231-004-0520-x
[3] Ali, Mohamed E. "Heat transfer characteristics of a continuous stretching surface." *Wärme-und Stoffübertragung* 29, no. 4 (1994): 227-234. https://doi.org/10.1007/BF01539754
[4] Pal, Dulal. "Mixed convection heat transfer in the boundary layers on an exponentially stretching surface with magnetic field." *Applied Mathematics and Computation* 217, no. 6 (2010): 2356-2369. https://doi.org/10.1016/j.amc.2010.07.035
[5] Aman, Fazlina, and Anuar Ishak. "Hydromagnetic flow and heat transfer adjacent to a stretching vertical sheet with prescribed surface heat flux." *Heat and Mass Transfer* 46 (2010): 615-620. https://doi.org/10.1007/s00231-010-0606-6
[6] Ibrahim, Wubshet, and B. Shanker. "Unsteady MHD boundary-layer flow and heat transfer due to stretching sheet in the presence of heat source or sink." *Computers & Fluids* 70 (2012): 21-28. https://doi.org/10.1016/j.compfluid.2012.08.019

[7] Mabood, F., and K. Das. "Melting heat transfer on hydromagnetic flow of a nanofluid over a stretching sheet with radiation and second-order slip." *The European Physical Journal Plus* 131 (2016): 1-12. https://doi.org/10.1140/epjp/i2016-16003-1
[8] Mukhopadhyay, Swati. "MHD boundary layer flow and heat transfer over an exponentially stretching sheet embedded in a thermally stratified medium." *Alexandria Engineering Journal* 52, no. 3 (2013): 259-265. https://doi.org/10.1016/j.aej.2013.02.003
[9] Mustafa, Meraj, Tasawar Hayat, Pop Ioan, and Awatif Hendi. "Stagnation-point flow and heat transfer of a Casson fluid towards a stretching sheet." *Zeitschrift für Naturforschung A* 67, no. 1-2 (2012): 70-76. https://doi.org/10.5560/zna.2011-0057
[10] Ramesh, G. K., B. C. Prasannakumara, B. J. Gireesha, and M. M. Rashidi. "Casson fluid flow near the stagnation point over a stretching sheet with variable thickness and radiation." *Journal of Applied Fluid Mechanics* 9, no. 3 (2016): 1115-1022. https://doi.org/10.18869/acadpub.jafm.68.228.24584
[11] Prakash, G. Balaji, G. V. Ramana Reddy, W. Sridhar, Y. Hari Krishna, and B. Mahaboob. "Thermal radiation and heat source effects on MHD Casson fluid over an oscillating vertical porous plate." *Journal of Computer and Mathematical Sciences* 10, no. 5 (2019): 1021-1031. https://doi.org/10.29055/jcms/1088
[12] Raju, C. S. K., N. Sandeep, V. Sugunamma, M. Jayachandra Babu, and JV Ramana Reddy. "Heat and mass transfer in magnetohydrodynamic Casson fluid over an exponentially permeable stretching surface." *Engineering Science and Technology, an International Journal* 19, no. 1 (2016): 45-52. https://doi.org/10.1016/j.jestch.2015.05.010
[13] Jaafar, A'isyah, Zanariah Mohd Yusof, Noraini Ahmad, and Anuar Jamaludin. "The Effects of Buoyancy, Magnetic Field and Thermal Radiation on the Flow and Heat Transfer due to an Exponentially Stretching Sheet." *CFD Letters* 15, no. 4 (2023): 1-16. https://doi.org/10.37934/cfdl.15.4.116
[14] Dandu, Sridevi, Venkata Ramana Murthy Chitrapu, and Udaya Bhaskara Varma Nadimpalli. "Radiation Absorption and Diffusion Thermo Effects on Unsteady MHD Casson Fluid Flow Past a Moving Inclined Plate Embedded in Porous Medium in the Presence of Chemical Reaction and Thermal Radiation." *Journal of Advanced Research in Applied Sciences and Engineering Technology* 32, no. 3 (2023): 92-107. https://doi.org/10.37934/araset.32.3.92107
[15] Kumar, Bavanasi Pradeep, and Sangapatnam Suneetha. "Numerical Investigation of Diffusion Thermo and Thermal Diffusion on MHD Convective Flow of Williamson Nanofluid on a Stretching Surface Through a Porous Medium in the Presence Chemical Reaction and Thermal Radiation." *Journal of Advanced Research in Fluid Mechanics and Thermal Sciences* 115, no. 2 (2024): 141-157. https://doi.org/10.37934/arfmts.115.2.141157
[16] Kataria, Hari R., and Harshad R. Patel. "Soret and heat generation effects on MHD Casson fluid flow past an oscillating vertical plate embedded through porous medium." *Alexandria Engineering Journal* 55, no. 3 (2016): 2125-2137. https://doi.org/10.1016/j.aej.2016.06.024
[17] Kodi, Raghunath, Obulesu Mopuri, Sujatha Sree, and Venkateswaraju Konduru. "Investigation of MHD Casson fluid flow past a vertical porous plate under the influence of thermal diffusion and chemical reaction." *Heat Transfer* 51, no. 1 (2022): 377-394. https://doi.org/10.1002/htj.22311
[18] Kumar, K. Kranthi, C. H. Baby Rani, and A. V. Papa Rao. "MHD Casson fluid flow along inclined plate with Hall and aligned magnetic effects." *Frontiers in Heat and Mass Transfer (FHMT)* 17 (2021). https://doi.org/10.5098/hmt.17.2
[19] Bejawada, Shankar Goud, Yanala Dharmendar Reddy, Wasim Jamshed, Kottakkaran Sooppy Nisar, Abdulaziz N. Alharbi, and Ridha Chouikh. "Radiation effect on MHD Casson fluid flow over an inclined non-linear surface with chemical reaction in a Forchheimer porous medium." *Alexandria Engineering Journal* 61, no. 10 (2022): 8207-8220. https://doi.org/10.1016/j.aej.2022.01.043
[20] Goud, B. Shankar, Y. Dharmendar Reddy, and Kanayo Kenneth Asogwa. "Chemical reaction, Soret and Dufour impacts on magnetohydrodynamic heat transfer Casson fluid over an exponentially permeable stretching surface with slip effects." *International Journal of Modern Physics B* 37, no. 13 (2023): 2350124. https://doi.org/10.1142/S0217979223501242
[21] Annapureddy, Damodara Reddy, Sarada Devi Puliyeddula, Nagaraju Vellanki, and Kalyan Kumar Palaparthi. "Heat and Mass Transfer in Unsteady Radiating MHD Flow of a Maxwell Fluid with a Porous Vertically Stretching Sheet in the Presence of Activation Energy and Thermal Diffusion Effects." *Journal of Advanced Research in Fluid Mechanics and Thermal Sciences* 115, no. 2 (2024): 158-177. https://doi.org/10.37934/arfmts.115.2.158177
[22] Thirupathi, Gurrala, Kamatam Govardhan, and Ganji Narender. "Radiative magnetohydrodynamics Casson nanofluid flow and heat and mass transfer past on nonlinear stretching surface." *Journal of Advanced Research in Numerical Heat Transfer* 6, no. 1 (2021): 1-21. https://doi.org/10.3762/bxiv.2021.65.v1
[23] Sulochana, C., S. Payad Samrat, and N. Sandeep. "Thermal radiation effect on MHD nanofluid flow over a stretching sheet." *International Journal of Engineering Research in Africa* 23 (2016): 89-102. https://doi.org/10.4028/www.scientific.net/JERA.23.89

[24] Makinde, O. D., and S. R. Mishra. "On stagnation point flow of variable viscosity nanofluids past a stretching surface with radiative heat." *International Journal of Applied and Computational Mathematics* 3 (2017): 561-578. https://doi.org/10.1007/s40819-015-0111-1
[25] Jalilpour, B., S. Jafarmadar, M. M. Rashidi, D. D. Ganji, R. Rahime, and A. B. Shotorban. "MHD non-orthogonal stagnation point flow of a nanofluid towards a stretching surface in the presence of thermal radiation." *Ain Shams Engineering Journal* 9, no. 4 (2018): 1671-1681. https://doi.org/10.1016/j.asej.2016.09.011
[26] Reddy, Yanala Dharmendar, B. Shankar Goud, M. Riaz Khan, Mohamed Abdelghany Elkotb, and Ahmed M. Galal. "Transport properties of a hydromagnetic radiative stagnation point flow of a nanofluid across a stretching surface." *Case Studies in Thermal Engineering* 31 (2022): 101839. https://doi.org/10.1016/j.csite.2022.101839
[27] Awang, Noorehan, Nurul Hidayah Ab Raji, Anis Athirah Rahim, Mohd Rijal Ilias, Sharidan Shafie, and Siti Shuhada Ishak. "Nanoparticle Shape Effects of Aligned Magnetohydrodynamics Mixed Convection Flow of Jeffrey Hybrid Nanofluid over a Stretching Vertical Plate." *Journal of Advanced Research in Applied Mechanics* 112, no. 1 (2024): 88-101. https://doi.org/10.37934/aram.112.1.88101
[28] Kumar, Vasa Vijaya, Mamidi Narsimha Raja Shekar, and Shankar Goud Bejawada. "Heat and Mass Transfer Significance on MHD Flow over a Vertical Porous Plate in the Presence of Chemical Reaction and Heat Generation." *CFD Letters* 16, no. 5 (2024): 9-20. https://doi.org/10.37934/cfdl.16.5.920
[29] Omar, Nur Fatihah Mod, Husna Izzati Osman, Ahmad Qushairi Mohamad, Rahimah Jusoh, and Zulkhibri Ismail. "Analytical solution of unsteady MHD casson fluid with thermal radiation and chemical reaction in porous medium." *Journal of Advanced Research in Applied Sciences and Engineering Technology* 29, no. 2 (2023): 185-194. https://doi.org/10.37934/araset.29.2.185194
[30] Vijayaragavan, R., and S. Karthikeyan. "Joule heating and thermal radiation effects on chemically reacting Casson fluid past a vertical plate with variable magnetic field." *Research Journal of Engineering and Technology* 8, no. 4 (2017): 393-404. https://doi.org/10.5958/2321-581X.2017.00070.8
[31] Ilias, Mohd Rijal, Nurul Nabilah Rosli, Siti Shuhada Ishak, Vincent Daniel David, Sharidan Shafie, and Mohd Nashriq Abd Rahman. "Radiation and Nanoparticles Shape Effect on Aligned MHD Jeffrey Hybrid Nanofluids Flow and Heat Transfer over a Stretching Inclined Plate." *Journal of Advanced Research in Applied Mechanics* 109, no. 1 (2023): 84-102. https://doi.org/10.37934/aram.109.1.84102
[32] Sekhar, P. Raja, S. Sreedhar, S. Mohammed Ibrahim, and P. Vijaya Kumar. "Radiative heat source fluid flow of MHD Casson nanofluid over a non-linear inclined surface with Soret and Dufour effects." *CFD Letters* 15, no. 7 (2023): 42-60. https://doi.org/10.37934/cfdl.15.7.4260
[33] Sarma, Gobburu Sreedhar, Ganji Narender, Dontula Shankaraiah, Vishwaroju Ramakrishna, and Gade Mallikarjun Reddy. "Analysis of Magneto Hydrodynamic Casson Nanofluid on an Inclined Porous Stretching Surface with Heat Source/Sink and Viscous Dissipation Effects: A Buongiorno Fluid Model Approach." *Journal of Advanced Research in Fluid Mechanics and Thermal Sciences* 109, no. 2 (2023): 151-167. https://doi.org/10.37934/arfmts.109.2.151167
[34] Swain, B. K., B. C. Parida, S. Kar, and N. Senapati. "Viscous dissipation and joule heating effect on MHD flow and heat transfer past a stretching sheet embedded in a porous medium." *Heliyon* 6, no. 10 (2020). https://doi.org/10.1016/j.heliyon.2020.e05338
[35] Sharma, B. K., and Rishu Gandhi. "Combined effects of Joule heating and non-uniform heat source/sink on unsteady MHD mixed convective flow over a vertical stretching surface embedded in a Darcy-Forchheimer porous medium." *Propulsion and Power Research* 11, no. 2 (2022): 276-292. https://doi.org/10.1016/j.jppr.2022.06.001
[36] Goud, Bejawada Shankar, Yanala Dharmendar Reddy, and Satyaranjan Mishra. "Joule heating and thermal radiation impact on MHD boundary layer Nanofluid flow along an exponentially stretching surface with thermal stratified medium." *Proceedings of the Institution of Mechanical Engineers, Part N: Journal of Nanomaterials, Nanoengineering and Nanosystems* 237, no. 3-4 (2023): 107-119. https://doi.org/10.1177/23977914221100961
[37] Goud, Bejawada Shankar, and Gurram Dharmaiah. "Role of Joule heating and activation energy on MHD heat and mass transfer flow in the presence of thermal radiation." *Numerical Heat Transfer, Part B: Fundamentals* 84, no. 5 (2023): 620-641. https://doi.org/10.1080/10407790.2023.2215917
[38] Goud, B. Shankar, Y. Dharmendar Reddy, V. Srinivasa Rao, and Zafar Hayat Khan. "Thermal Radiation and Joule heating effects On a Magnetohydrodynamic Casson Nanofluid glow in the presence of chemical reaction through a non-linear inclined porous stretching sheet." *Journal of Naval Architecture & Marine Engineering* 17, no. 2 (2020). https://doi.org/10.3329/jname.v17i2.49978
[39] Reddy, M. Vinodkumar, K. Vajravelu, P. Lakshminarayana, and G. Sucharitha. "Heat source and Joule heating effects on convective MHD stagnation point flow of Casson nanofluid through a porous medium with chemical reaction." *Numerical Heat Transfer, Part B: Fundamentals* 85, no. 3 (2024): 286-304. https://doi.org/10.1080/10407790.2023.2233694

[40] Krishna, M. Veera, N. Ameer Ahammad, and Ali J. Chamkha. "Radiative MHD flow of Casson hybrid nanofluid over an infinite exponentially accelerated vertical porous surface." *Case Studies in Thermal Engineering* 27 (2021): 101229. https://doi.org/10.1016/j.csite.2021.101229

[41] Krishna, M. Veera, Kamboji Jyothi, and Ali J. Chamkha. "Heat and mass transfer on MHD flow of second-grade fluid through porous medium over a semi-infinite vertical stretching sheet." *Journal of Porous Media* 23, no. 8 (2020). https://doi.org/10.1615/JPorMedia.2020023817

[42] Pramanik, S. "Casson fluid flow and heat transfer past an exponentially porous stretching surface in presence of thermal radiation." *Ain Shams Engineering Journal* 5, no. 1 (2014): 205-212. https://doi.org/10.1016/j.asej.2013.05.003

[43] Ishak, Anuar, Roslinda Nazar, and Ioan Pop. "Flow and heat transfer characteristics on a moving flat plate in a parallel stream with constant surface heat flux." *Heat and Mass Transfer* 45 (2009): 563-567. https://doi.org/10.1007/s00231-008-0462-9